Structures and Related Properties of AgX Bearing 3,3′-Thiobispyridine ($X^- = NO_3^-$, BF_4^-, ClO_4^-, and PF_6^-)

Ok-Sang Jung,*,† Yun Ju Kim,† Young-A Lee,† Hee K. Chae,‡ Ho G. Jang,§ and Jongki Hong||

Materials Chemistry Laboratory, Korea Institute of Science and Technology, Seoul 136-791, Korea, Department of Chemistry, Hankuk University of Foreign Studies, Yongin 449-791, Korea, Department of Chemistry, Korea University, Seoul 136-701, Korea, and Korea Basic Research Institute, Taejon 305-600, Korea

Received September 21, 2000

Infinite molecular helices [Ag(3,3′-Py_2S)]X (3,3′-Py_2S = 3,3′-thiobispyridine; $X^- = BF_4^-$, ClO_4^-, and PF_6^-) have been rationally constructed or induced. Crystallographic characterization ($X^- = BF_4^-$, monoclinic $P2_1/n$, a = 8.946(3) Å, b = 14.130(2) Å, c = 10.124(2) Å, β = 107.83(2)°, V = 1218.3(5) Å^3, Z = 4, R = 0.0351; $X^- = ClO_4^-$, monoclinic $P2_1/n$, a = 8.884(1) Å, b = 14.305(3) Å, c = 10.110(1) Å, β = 106.78(1)°, V = 1230.1(3) Å^3, Z = 4, R = 0.0417; $X^- = PF_6^-$, monoclinic $P2_1/c$, a = 10.959(2) Å, b = 9.808(2) Å, c = 14.065(3) Å, β = 112.03(2)°, V = 1401.4(5) Å^3, Z = 4, R = 0.0442) reveals that the skeletal structure is an oblong cylindrical cationic helix consisting of alternating Ag(I) and 3,3′-Py_2S species and that its counteranions are pinched in two columns inside each helix. The formation of the helical coordination polymer appears to be primarily associated with a suitable combination of the skewed conformer of 3,3′-Py_2S and the potential linear geometry of the N−Ag(I)−N bond. However, the framework of the nitrate analogue [Ag(3,3′-Py_2S)NO_3] (monoclinic $P2_1/c$, a = 8.177(2) Å, b = 10.291(1) Å, c = 14.771(2) Å, β = 102.19(1)°, V = 1214.9(4) Å^3, Z = 4, R = 0.0300) is a two-dimensional network consisting of an 18-membered ring unit, where each 3,3′-Py_2S acts as a N,N′,S− tridentate ligand connecting three tetrahedral silver(I) ions with the monodentate nitrate weakly bonded to the silver (Ag···O = 2.65(1) Å) rather than acting as a counteranion. The anion exchange of [Ag(3,3′-Py_2S)NO_3] with BF_4^-, ClO_4^-, or PF_6^- has been accomplished in aqueous media. The two-dimensional networks are easily converted into the helices via the anion exchange, but the reverse anion exchange proceeds slightly. Thermal analyses indicate a relationship between the thermal stabilities and the structural properties.

Introduction

The induction of naturally occurring helical motifs is now of great interest since the motif has been found to be a fundamental structure of proteins, nucleic acids, and oligosaccharides.[1−3] Several approaches for the generation of helical entities have been pursued, the product of materials having applications such as templating precursors,[4] memory devices,[5,6] and biomimetics[7,8] in areas of chirotechnology,[9] DNA mimics,[10] nonlinear optics,[11] and structural biology.[12] Such a helical topology has been designed and assembled by the selection of basic components such as the coordination geometry of metal ions, the binding site of donating atoms, and the length of spacers.[8,9,13−15] Various ligands have been investigated as molecular helical building blocks,[13] but the synthesis of a suitable helical frame still remains unpredictable presumably because of the presence of weak induced intra- or intermolecular interactions.

We previously reported that the reaction of 3,3′-oxybispyridine (3,3′-Py_2O) with AgX results in the formation of cylindrical helices and that the helices reversibly stretch via counteranion exchange.[16] However, exploitation of 3,3′-thiobispyridine (3,3′-Py_2S) as a spacer has not been attempted. The 3,3′-thiobispyridine ligand possesses a key tectonic helical element, that is,

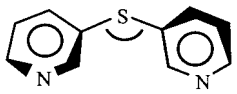

3,3'-Py_2S

* To whom correspondence should be addressed. Fax: 82-2-958-5089. E-mail: oksjung@kist.re.kr.
† Korea Institute of Science and Technology.
‡ Hankuk University of Foreign Studies.
§ Korea University.
|| Korea Basic Research Institute.

(1) Guccia, L. A.; Lehn, J.-M.; Homo, J. C.; Shumutz, M. *Angew. Chem., Int. Ed.* **2000**, *39*, 233−237.
(2) Prince, R. B.; Brunsveld, L.; Meijer, E. W.; Moore. J. S. *Angew. Chem., Int. Ed.* **2000**, *39*, 228−230.
(3) Rowan, A. E.; Nolte, R. J. M. *Angew. Chem., Int. Ed.* **1998**, *37*, 63−68.
(4) Dietrich-Bucheker, C. O.; Guilhem, J.; Pascard, C.; Sauvage, J.-P. *Angew. Chem., Int. Ed. Engl.* **1990**, *29*, 1154−1156.
(5) Yashima, E.; Maeda, K.; Okamoto, Y. *Nature* **1999**, *399*, 449−451.
(6) Piguet, C.; Bernardinelli, G.; Hopfgartner, G. *Chem. Rev.* **1997**, *97*, 2005−2062.
(7) Hannak, R. B.; Färber, G.; Konrat, R.; Kräutler, B. *J. Am. Chem. Soc.* **1997**, *119*, 2313−2314.
(8) Orr, G. W.; Barbour, L. J.; Atwood, J. L. *Science* **1999**, *285*, 1049−1052.
(9) Biradha, K.; Seward, C.; Zaworotko, M. J. *Angew. Chem., Int. Ed.* **1999**, *38*, 492−494.
(10) Chalmers, R.; Guhathakurta, A.; Benjamin, H.; Kleckner, N. *Cell* **1998**, *93*, 897−908.
(11) Kauranen, M.; Verviest, T.; Bouttoon, C.; Teerenstra, M. N.; Clays, K.; Schouten, A. J.; Nolte, R. J. M.; Pearsons, A. *Science* **1995**, *270*, 966−969.
(12) Klug, A. *Angew. Chem., Int. Ed. Engl.* **1983**, *22*, 565−582.
(13) Constable, E. C. *Tetrahedron* **1992**, *48*, 10013−10059.
(14) Carlucci, L.; Ciani, G.; Proserpio, D. M.; Sironi, A. *Inorg. Chem.* **1998**, *37*, 5941−5943.
(15) Lehn, J.-M.; Rigault, A.; Siegel, J.; Harrowfield, J.; Chevrier, B.; Moras, D. *Proc. Natl. Acad. Sci. U.S.A.* **1987**, *84*, 2565−2569.

10.1021/ic001072u CCC: $20.00
Published on Web 03/28/2001

Table 1. Crystallographic Data for [Ag(3,3′-Py_2S)NO_3], [Ag(3,3′-Py_2S)]BF_4, [Ag(3,3′-Py_2S)]ClO_4, and [Ag(3,3′-Py_2S)]PF_6

	[Ag(3,3′-Py_2S)NO_3]	[Ag(3,3′-Py_2S)]BF_4	[Ag(3,3′-Py_2S)]ClO_4	[Ag(3,3′-Py_2S)]PF_6
formula	$C_{10}H_8AgN_3O_3S$	$C_{10}H_8Ag\ BF_4N_2S$	$C_{10}H_8AgClN_2O_4S$	$C_{10}H_8Ag\ F_6N_2PS$
fw	358.12	382.92	395.56	441.08
space group	$P2_1/c$	$P2_1/n$	$P2_1/n$	$P2_1/c$
a, Å	8.177(2)	8.946(3)	8.884(1)	10.959(2)
b, Å	10.291(1)	14.130(2)	14.305(3)	9.808(2)
c, Å	14.771(2)	10.124(2)	10.110(1)	14.065(3)
β, deg	102.19(1)	107.83(2)	106.78(1)	112.03(2)
V, Å^3	1214.9(4)	1218.3(5)	1230.1(3)	1401.4(5)
Z	4	4	4	4
d_{calcd}, g cm^{-3}	1.958	2.088	2.136	2.091
μ, mm^{-1}	1.833	1.860	2.035	1.761
R [a] $\{I > 2\ \sigma(I)\}$	R1 = 0.0300 wR2 = 0.0729	R1 = 0.0351 wR2 = 0.0906	R1 = 0.0417 wR2 = 0.1039	R1 = 0.0442 wR2 = 0.1157

[a] $R1 = \sum||F_o| - |F_c||/\sum|F_o|$. $wR2 = (\sum w(F_o^2 - F_c^2)^2/\sum wF_o^2)^{1/2}$.

the skewed conformer with nonrigid interannular dihedral angles between two 3-pyridyl groups,[17] in contrast to 4,4′-thiobispyridine.[18−20] Silver(I) ion can be employed as a linear geometric metal because it has been known to preferably exhibit linear or T-shaped stereochemistry.[19,21]

To scrutinize subtle differences in bonding effects between the 3,3′-Py_2S and 3,3′-Py_2O helical units, we describe here studies on the helical structure of [Ag(3,3′-Py_2S)]X ($X^- = BF_4^-$, ClO_4^-, and PF_6^-) and on the induction of the helical structure via an anion exchange. Nitrate, tetrafluoroborate, perchlorate, and hexafluorophosphate that frequently appear in chemistry, environmental pollution, disease pathways, and biological processes[22,23] were selected as the anionic balancer for the cationic helical skeleton.

Experimental Section

Materials and Physical Measurements. AgX and NaX ($X^- = NO_3^-$, BF_4^-, ClO_4^-, and PF_6^-) were purchased from Strem and Junsei Chemical Co., respectively, and were used without further purification. 3,3′-Thiobispyridine (3,3′-Py_2S) was prepared according to the literature procedure.[24] Elemental microanalyses (C, H, N) were performed on crystalline samples by the Advanced Analysis Center at KIST using a Perkin-Elmer 2400 CHNS analyzer. X-ray powder diffraction data were recorded on a Rigaku RINT/DMAX-2500 diffractometer at 40 kV, 126 mA for Cu Kα. Thermal analyses were carried out under a dinitrogen atmosphere at a scan rate of 10 °C/min using a Stanton Red Croft TG 100. Infrared spectra were obtained on a Perkin-Elmer 16F PC FTIR spectrophotometer with samples prepared as KBr disks.

Preparation of [Ag(3,3′-Py_2S)NO_3]. A methanolic solution (5 mL) of 3,3′-Py_2S (56 mg, 0.3 mmol) was slowly diffused into an aqueous solution (5 mL) of $AgNO_3$ (51 mg, 0.3 mmol). Colorless crystals of [Ag(3,3′-Py_2S)NO_3] suitable for crystallographic characterization were formed at the interface and were obtained in 3 days in 82% yield. Anal. Calcd for $C_{10}H_8N_3O_3SAg$: C, 33.5; H, 2.3; N, 11.7. Found: C, 33.4; H, 2.2; N, 11.4. IR (cm^{-1}): $\nu(NO_3)$, 1378 (s).

Preparation of [Ag(3,3′-Py_2S)]BF_4. The diffusion of a methanolic solution of Py_2S with an aqueous solution of $AgBF_4$ afforded colorless crystals of [Ag(3,3′-Py_2S)]BF_4. Yield: 79%. Anal. Calcd for $C_{10}H_8N_2BF_4SAg$: C, 31.4; H, 2.1; N, 7.3. Found: C, 31.3; H, 2.1; N, 7.1. IR (cm^{-1}): $\nu(BF_4)$, 1058 (s, br).

Preparation of [Ag(3,3′-Py_2S)]ClO_4. The reaction of an ethanolic solution of 3,3′-Py_2S with an aqueous solution of $AgClO_4$ gave colorless crystals of [Ag(3,3′-Py_2S)]ClO_4. Yield: 80%. Anal. Calcd for $C_{10}H_8N_2O_4SClAg$: C, 30.4; H, 2.0; N, 7.1. Found: C, 30.3; H, 2.0; N, 7.0. IR (cm^{-1}): $\nu(ClO_4)$, 1092 (s, br).

Preparation of [Ag(3,3′-Py_2S)]PF_6. The similar treatment of a solution of 3,3′-Py_2S in acetone with an aqueous solution of $AgPF_6$ resulted in [Ag(3,3′-Py_2S)]PF_6. Yield: 82%. Anal. Calcd for $C_{10}H_8N_2PF_6SAg$: C, 27.2; H, 1.8; N, 6.4. Found: C, 27.2; H, 1.8; N, 6.4. IR (cm^{-1}): $\nu(PF_6)$, 834 (s, br).

Anion Exchange of [Ag(3,3′-Py_2S)NO_3] with $NaPF_6$. An aqueous solution (5 mL) of $NaPF_6$ (51 mg, 0.3 mmol) was added to a suspension of microcrystalline [Ag(3,3′-Py_2S)NO_3] (36 mg, 0.1 mmol) in water (5 mL) at room temperature. The reaction mixture was stirred, and each precipitate after 1, 3, and 6 h was monitored by IR spectroscopy. After 6 h, the reaction mixture was filtered and washed with several aliquots of water and methanol. Elemental analysis, the IR spectrum, and the X-ray powder diffraction pattern of the exchanged species were identical with those of [Ag(3,3′-Py_2S)]PF_6 prepared by the direct diffusion of $AgPF_6$ with 3,3′-Py_2S.

Counteranion Exchange of [Ag(3,3′-Py_2S)]BF_4 with $NaPF_6$. An aqueous solution (5 mL) of $NaPF_6$ (51 mg, 0.3 mmol) was added to an aqueous suspension (5 mL) of microcrystalline [Ag(3,3′-Py_2S)]BF_4 (38 mg, 0.1 mmol) at room temperature. The reaction mixture was stirred, and each precipitate was monitored after 1, 3, 6, and 12 h by IR spectroscopy. After 12 h, the reaction mixture was filtered and washed with several aliquots of water and methanol. Elemental analysis and the X-ray powder diffraction pattern are consistent with those for [Ag(3,3′-Py_2S)]PF_6 prepared by the anion exchange of [Ag(3,3′-Py_2S)NO_3] with $NaPF_6$ as well as that of [Ag(3,3′-Py_2S)]PF_6 prepared by the slow diffusion of $AgPF_6$ with 3,3′-Py_2S.

Crystallographic Structure Determinations. All X-ray data were collected on an Enraf-Nonius CAD4 automatic diffractometer with graphite-monochromated Mo Kα radiation ($\lambda = 0.710\ 73$ Å) at ambient temperature. Unit cell dimensions were based on 25 well-centered reflections by using a least-squares procedure. All crystals were formed in the monoclinic crystal system. During the data collection, three standard reflections monitored after every hour did not reveal any systematic variation in intensity. The data were corrected for Lorentz and polarization effects. Absorption effects were corrected by the empirical ψ-scan method. The structures were solved by the Patterson method (SHELXS 97) and refined by full-matrix least-squares techniques (SHELXL 97).[25] The non-hydrogen atoms were refined anisotropically, and hydrogen atoms were placed in calculated positions and refined only for the isotropic thermal factors. Crystal parameters and procedural information corresponding to data collection and structure refinement are given in Table 1. Tables listing atom

(16) Jung, O.-S.; Kim, Y. J.; Lee, Y.-A.; Park, J. K.; Chae, H. K. *J. Am. Chem. Soc*. **2000**, *122*, 9921−9925.
(17) Dunne, S. J.; Summers, L. A.; von Nagy-Felsobuki, E. I. *J. Heterocycl. Chem.* **1992**, *29*, 851−858.
(18) Jung, O.-S.; Park, S. H.; Kim, D. C.; Kim, K. M. *Inorg. Chem*. **1998**, *37*, 610−611.
(19) Jung, O.-S.; Park, S. H.; Park, C. H.; Park, J. K. *Chem. Lett*. **1999**, 923−924.
(20) Jung, O.-S.; Park, S. H.; Lee, Y.-A.; Lee, U. *Chem. Lett*. **2000**, 1012−1013.
(21) Carlucci, L. C.; Ciani, G.; Gudenberg, D. W. V.; Proserpio, D. M. *Inorg. Chem*. **1997**, *36*, 3812−3813.
(22) Schmidtchen, F. P.; Berger, M. *Chem. Rev*. **1997**, *97*, 1609−1646.
(23) Beer, P. D. *Acc. Chem. Res.* **1998**, *31*, 71−80.
(24) Summers, L. A. *J. Heterocycl. Chem.* **1987**, *24*, 533−544.
(25) Sheldrick, G. M. *SHELXS-97: A Program for Structure Determination*; University of Göttingen: Göttingen, Germany, 1997. Sheldrick, G. M. *SHELXL-97: A Program for Structure Refinement*; University of Göttingen: Göttingen, Germany, 1997.

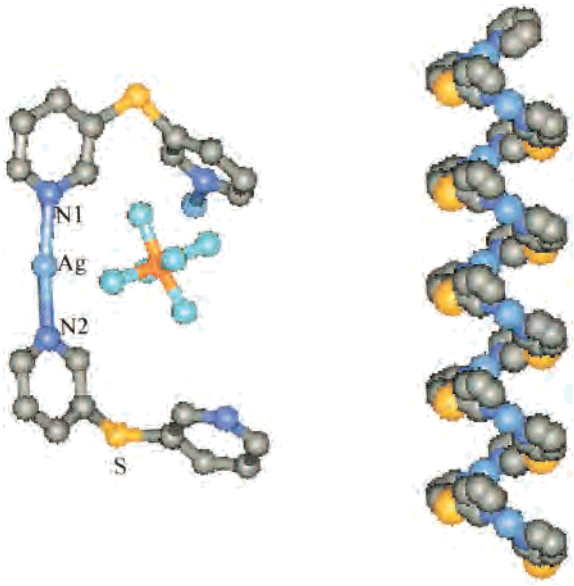

Figure 1. Asymmetric unit showing the 50% probability thermal ellipsoids (left) and infinite space-filling representation (right) of [Ag(3,3′-Py_2S)]PF_6. Light blue, yellow, orange, blue, gray, and green correspond to Ag, S, P, N, C, and F atoms, respectively. For the infinite space filling, the PF_6^- counteranions were omitted for clarity.

positions, anisotropic displacement parameters, and hydrogen atom locations for the four structure determinations are available as Supporting Information.

Results

Construction. Our primary strategy employed is the propagation of a potential linear coordination geometric Ag(I) unit via the skewed conformer of the 3,3′-Py_2S bidirectional spacer. The slow diffusion of a methanolic solution of 3,3′-Py_2S into an aqueous solution of AgX ($X^- = NO_3^-$, BF_4^-, ClO_4^-, and PF_6^-) afforded single crystals of the 1:1 adducts (Ag/3,3′-Py_2S) in high yields. The reactions based on this design strategy resulted in self-assembly of the cylindrical helices, but the same treatment of $AgNO_3$ with 3,3′-Py_2S gave the two-dimensional network. Each structure was not significantly affected by the change of the mole ratio and the concentration. Moreover, when acetone or ethanol was used as solvent instead of methanol, the same products were obtained. The compounds are insoluble in water and common organic solvents but are stable for several days in a pH 3.5−9.0 aqueous suspension.

Crystal Structures. Asymmetric unit and infinite molecular structure of [Ag(3,3′-Py_2S)]PF_6 are depicted in Figure 1, and selected bond distances and angles are listed in Table 2. Its skeletal structure is a single stranded helix consisting of alternating Ag(I) and 3,3′-Py_2S, and there are two units in each turn (2_1 along the *b* axis). The oblong cylindrical helices (the shortest intrahelical Ag···Ag, 7.28 Å, times the shortest intrahelical S···S, 10.02 Å) are arrayed in an alternating right-handed and left-handed fashion. Their counteranions are pinched in two columns between/inside the helical pitch presumably because of the presence of the weak electrostatic interactions with the Ag(I) cations (the shortest Ag···F is 3.06 Å). The structures of [Ag(3,3′-Py_2S)]BF_4 and [Ag(3,3′-Py_2S)]ClO_4 are basically similar, and thus, the structure of [Ag(3,3′-Py_2S)]ClO_4 is shown in Figure 2. The skeletal structure of [Ag(3,3′-Py_2S)]ClO_4 is similar to that of [Ag(3,3′-Py_2S)]PF_6, but the helical pitches (14.130(2) Å for [Ag(3,3′-Py_2S)]BF_4; 14.305(2) Å for [Ag(3,3′-Py_2S)]ClO_4) are much longer than that of [Ag(3,3′-Py_2S)]PF_6 (9.808(2) Å). The bond angles of C−S−C are smaller than those of C−O−C in the corresponding 3,3′-Py_2O analogue.[16] Another feature is the interhelical Ag···Ag distances (3.1221(8)−3.222(1) Å), which are shorter than the known ligand-unsupported closed-shell d^{10} Ag···Ag interactions.[26] The slightly bent angles of N−Ag−N (171.0(1)−173.3(1)°) support the presence of the weak metal−metal interactions. Thus, the stereochemistry around the silver ion may be best described as "an italic *T*" shape.

X-ray crystallographic characterization reveals that the [Ag(3,3′-Py_2S)NO_3] structure consists of a two-dimensional network (Figure 3). Selected bond lengths and angles are listed in Table 2. Each 3,3′-Py_2S acts as N,N′,S tridentate ligand connecting three tetrahedral silver(I) ions defining the skeleton of an 18-membered ring (7.5 × 8.1 Å). The local geometry of the silver(I) ion is a very distorted tetrahedron in order to sustain the molecular network (N(2)−Ag−S(1) = 151.52(8)°). The nitrate anion is weakly bonded to the silver(I) ion in a monodentate mode as a fourth ligand (Ag···O(1) = 2.65(1) Å) rather than as a counteranion. The Ag−N(1) and Ag−N(2) distances of 2.399(3) and 2.345(3) Å, respectively, are much longer than the corresponding bonds of the helical structures. For the network structure, one pyridyl group is rotated with respect to the other pyridyl group (dihedral angle 78.2(2)°), contrasting with 18.1(3)° in the helical structure. The Ag−S(1) distance (2.697(1) Å) is comparable to the corresponding bond in [Ag_3(NO_3)$_3$(Py_2S)$_2$·$2H_2O$].[19]

Anion Exchange. The counteranion exchange of [Ag(3,3′-Py_2O)]X with X^- ($X^- = BF_4^-$, ClO_4^-, and PF_6^-) smoothly occurs in a typical aqueous media. For [Ag(3,3′-Py_2S)]BF_4, the BF_4^- anions within the helix were completely exchanged with the octahedral PF_6^- anions. To investigate the exchange procedure, the counteranion exchange could be monitored by the characteristic IR bands of the counteranions.[20,27] The exchange in aqueous media at room temperature was checked after 1, 3, 6, and 12 h (Figure 4a). The infrared spectra show the gradual disappearance of intense BF_4^- bands (1058 cm^{-1}) and the appearance and growth of new PF_6^- bands (834 cm^{-1}). The BF_4^- peaks disappear completely after 12 h. The other peaks of the spectrum remain virtually unchanged, suggesting the same skeletal structure during and after the anion exchange process. The anion exchange of the network structural [Ag(3,3′-Py_2S)NO_3] unit with PF_6^- was easily accomplished (Scheme 1), indicating that the weakly bonded NO_3^- is labile enough to be exchanged with PF_6^- in aqueous suspension. The anion exchange was completed within 6 h (Figure 4b). In contrast to the counteranion exchange of [Ag(3,3′-Py_2S)]BF_4 with PF_6^-, the slight change of pyridyl peaks around 1500 cm^{-1} is ascribed to the change of skeletal structure via the anion exchange. The most interesting feature is that the elemental analysis and IR spectra of the exchanged species are coincident with those of the sample obtained by the counteranion exchange of [Ag(3,3′-Py_2S)]BF_4 with PF_6^-, indicating the formation of the same compound through the two different procedures. The X-ray powder diffraction patterns of the two procedural samples (Supporting Information) are the same, and furthermore, the position and intensity of peaks in the two powder patterns are similar to those of [Ag(3,3′-Py_2S)]PF_6 prepared via the direct diffusion. For the two exchanged samples, the high-angle peaks ($2\theta > 40°$) do not appear to be due to the intrinsic low-crystalline samples after the anion exchange. The reverse

(26) Singh, K.; Long, J. R.; Stavropoulos, P. *J. Am. Chem. Soc*. **1997**, *119*, 2942−2943.
(27) Yaghi, O. M.; Li, H. *J. Am. Chem. Soc*. **1996**, *118*, 295−296.

Table 2. Selected Bond Lengths (Å) and Angles (deg) for [Ag(3,3′-Py_2S)NO_3], [Ag(3,3′-Py_2S)]BF_4, [Ag(3,3′-Py_2S)]ClO_4, and [Ag(3,3′-Py_2S)]PF_6

	[Ag(3,3′-Py_2S)NO_3]	[Ag(3,3′-Py_2S)]BF_4	[Ag(3,3′-Py_2S)]ClO_4	[Ag(3,3′-Py_2S)]PF_6
Ag−N(1)	2.399(3)	2.145(3)	2.156(4)	2.136(4)
Ag−N(2)	2.354(3)	2.145(3)	2.163(4)	2.144(4)
Ag−S′	2.697(1)			
Ag−O(3)	2.652(2)			
Ag···Ag′		3.138(1)	3.1221(8)	3.222(1)
N(1)−Ag−N(2)	107.4(1)	172.7(1)	171.0(1)	173.3(1)
N(1)−Ag−S(1)′	100.55(9)			
N(2)−Ag−S(1)′	151.52(8)			
C−S−C	103.7(2)	105.6(2)	105.8(2)	105.0(2)

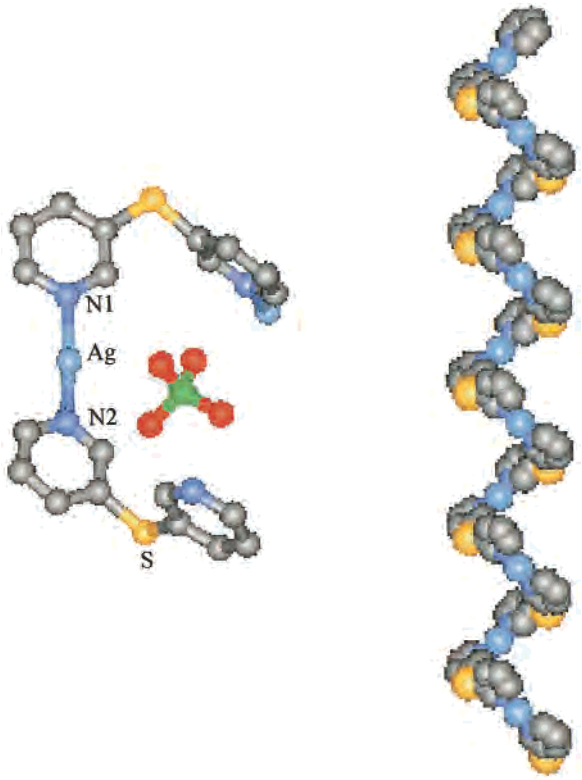

Figure 2. Asymmetric unit showing 50% probability thermal ellipsoids (left) and infinite space-filling representation (right) of [Ag(3,3′-Py_2S)]-ClO_4. Light blue, yellow, green, red, blue, and gray correspond to Ag, S, Cl, O, N, and C atoms, respectively. For the infinite space filling, the ClO_4^- counteranions were omitted for clarity.

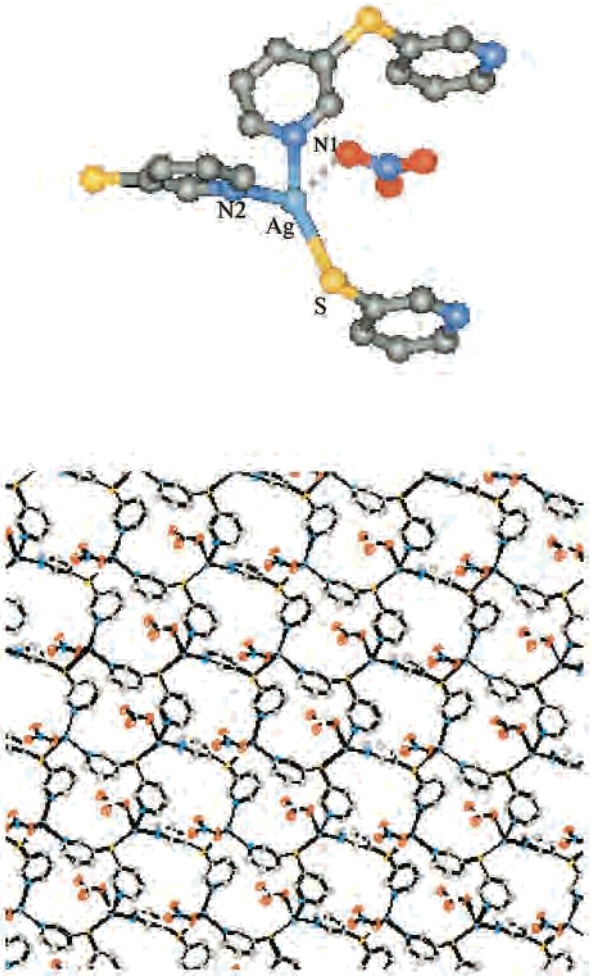

Figure 3. Asymmetric unit showing 50% probability thermal ellipsoids (top) and a top view of the infinite 2-D network (bottom) of [Ag(3,3′-Py_2S)NO_3].

exchange of [Ag(3,3′-Py_2S)]PF_6 with BF_4^- is very slow. Thus, the anion exchangeability is dependent on the anions, the reaction temperature, the reactant stoichiometry, and the concentration. The counteranion exchange of [Ag(3,3′-Py_2S)]ClO_4 with BF_4^- scarcely occurs at room temperature. The exchange of [Ag(3,3′-Py_2S)]ClO_4 with NO_3^- or PF_6^- proceeds slightly. The overall anion exchangeability seems to be governed by the nature of the anions rather than the skeletal structure.

Thermal Analysis. The thermal analyses have been used to establish a relationship between structure and properties.[18,28] The thermogravimetric traces are shown in Figure 5. The thermal stability of [Ag(3,3′-Py_2S)]X (X = BF_4^-, ClO_4^-, and PF_6^-) is variable (92−320 °C) even though the compounds have similar helical structures. The decomposition temperatures of [Ag(3,3′-Py_2S)]BF_4 (92 °C) and [Ag(3,3′-Py_2S)]ClO_4 (121 °C) are much lower than that of [Ag(3,3′-Py_2S)]PF_6 (320 °C). Moreover, the two compounds are thermally much more unstable than the corresponding 3,3′-Py_2O analogues (322 and 330 °C).[16] However, the decomposition temperature of [Ag(3,3′-Py_2S)]PF_6 (320 °C) is very similar to the 3,3′-Py_2O analogue (332 °C).[16] The thermal stability can be explained in terms of the structural properties. That is, the helical pitch of [Ag(3,3′-Py_2S)]PF_6 is similar to that of [Ag(3,3′-Py_2O)]PF_6, while the helical pitches of [Ag(3,3′-Py_2S)]BF_4 and [Ag(3,3′-Py_2S)]ClO_4 are much longer than those of the 3,3′-Py_2O analogues. Thus, the thermal stability seems to be attributed to the nature of the skeletal structures rather than to the anions. Such thermal properties indicate that the volume expansion due to thermal energy collapses the unreasonable helical pitch, resulting in the change from the highly ordered arrangement to the more random state. The [Ag(3,3′-Py_2S)NO_3] comprising the network structure is stable up to 162 °C.

(28) Jung, O.-S.; Park, S. H.; Kim, K. M.; Jang, H. G. *Inorg. Chem.* **1998**, *37*, 5781−5785.

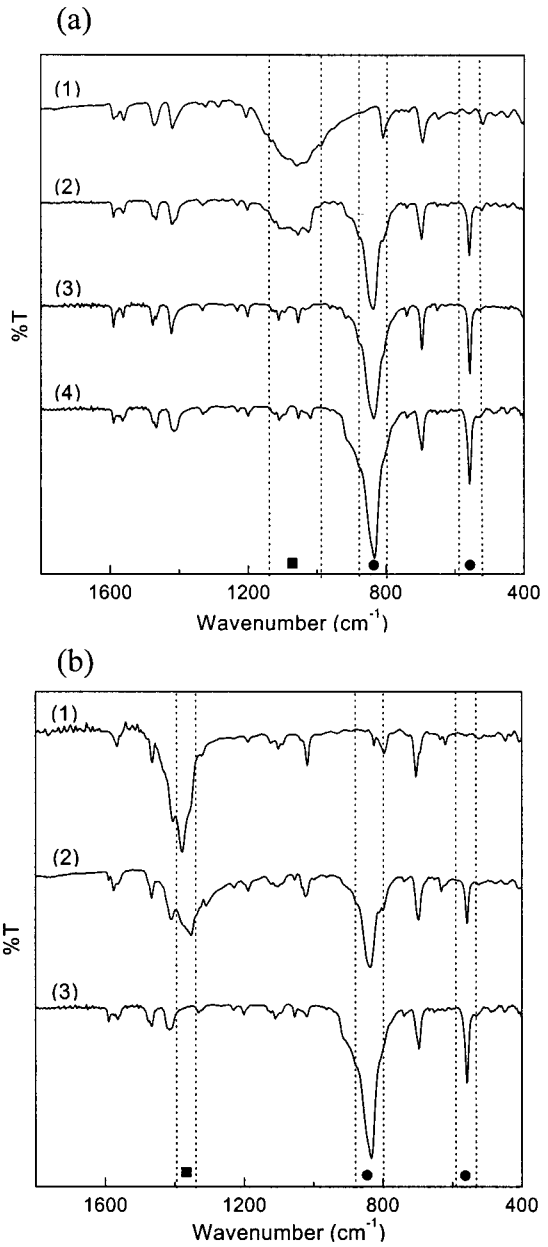

Figure 4. (a) IR (KBr pellet) change procedure during the counteranion exchange of [Ag(3,3′-Py_2S)]BF_4 with $NaPF_6$ after 1 h (1), 3 h (2), 6 h (3), and 12 h (4). ■ and ● denote BF_4 and PF_6 bands, respectively. (b) IR (KBr pellet) change procedure during the anion exchange of [Ag(3,3′-Py_2S)NO_3] with $NaPF_6$ after 1 h (1), 3 h (2), and 6 h (3). ■ and ● denote NO_3 and PF_6 bands, respectively.

Scheme 1

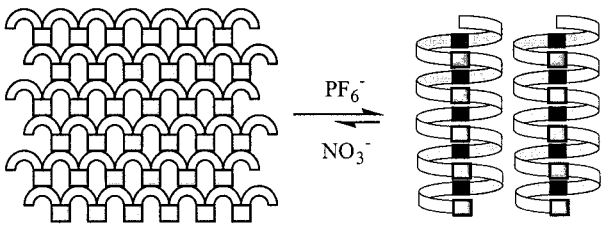

Discussion

A suitable combination of the skewed conformer of 3,3′-Py_2S and the linear geometry of the N−Ag(I)−N bond may contribute to a driving force for the formation of the infinite cylindrical helical molecules. The helices were efficiently constructed

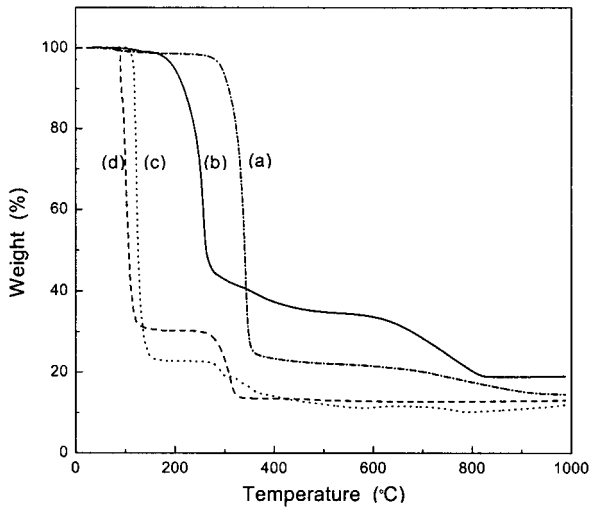

Figure 5. TGA traces of [Ag(3,3′-Py_2S)]PF_6 (a), [Ag(3,3′-Py_2S)NO_3] (b), [Ag(3,3′-Py_2S)]ClO_4 (c), and [Ag(3,3′-Py_2S)]BF_4 (d), each recorded at a heating rate of 10 °C min^{-1}.

irrespective of the reactant stoichiometry, solvent type, and concentration. Even though the size of the pinched anion, PF_6^-, is larger than BF_4^- and ClO_4^-, the helical pitches of [Ag(3,3′-Py_2S)]BF_4 and [Ag(3,3′-Py_2S)]ClO_4 are much longer than the pitch of [Ag(3,3′-Py_2S)]PF_6. These structural properties may be ascribed to the intrinsic properties of the 3,3′-Py_2S ligand: the conformational energy barrier of 3,3′-Py_2S is lower than that of 3,3′-Py_2O,[17,29,30] and furthermore, the C−S−C angle is contracted relative to the corresponding C−O−C angle in 3,3′-Py_2O. Thus, the crystal packing may be an important factor for the determination of the helical pitch rather than the volume of the counteranion. Although the helical pitch of [Ag(3,3′-Py_2S)]X ($X^- = BF_4^-$, ClO_4^-) is much longer than that of [Ag(3,3′-Py_2S)]-PF_6, the calculated crystal densities (shown in Table 1) are nearly invariant. Such a fact indicates that each helix of [Ag(3,3′-Py_2S)]X ($X^- = BF_4^-$, ClO_4^-) is interdigited. The short interhelical Ag···Ag distances relative to that of [Ag(3,3′-Py_2S)]-PF_6 gives evidence for the interdigited packing. The formation of the unique 2-D networks, [Ag(3,3′-Py_2S)NO_3], appears to be primarily associated with the properties of the anion. The coordinating nature of NO_3^- is an obstacle in the construction of the helix. Moreover, from the hard/soft acid−base concept, the soft sulfur donor of 3,3′-Py_2S may coordinate to the soft Ag(I). Actually, [Ag(3,3′-Py_2S)NO_3] has a Ag−S bond in contrast to that of the 3,3′-Py_2O analogue.[16]

The counteranions within the helices could be exchanged in aqueous media. The labile anion of the network [Ag(3,3′-Py_2S)-NO_3] is easily exchanged, followed by the dissociation of the weak Ag−S bond to restore the helical structure. The slow exchange of [Ag(3,3′-Py_2S)]PF_6 with NO_3^- is not completed even though the mole ratio (NO_3^-/[Ag(3,3′-Py_2S)]PF_6) increases. Though all experiments including the preparation and the anion exchange are carried out either in aqueous solutions or in aqueous suspensions, the infinite cationic molecules contain no solvate water molecules. This is presumably due to the intrinsic properties of the hydrophobic 3,3′-Py_2S skeletal structure. The high calculated densities for the crystals (ρ_{calcd} = 1.96−2.14) are indicative of tightly packed structures, indicating that there are no cavities that are large enough to accommodate guest

(29) Dunne, S. J.; Summers, L. A.; von Nagy-Felsobuki, E. I. *J. Mol. Struct.* **1992**, *268*, 373−388.
(30) Dunne, S. J.; Summers, L. A.; von Nagy-Felsobuki, E. I. *J. Mol. Struct.: THOECHEM* **1991**, *230*, 219−234.

molecules such as methanol and water. This is consistent with the thermochemical investigations, which show no weight loss of solvent molecules. The most salient feature is that such an interconversion via anion exchange may be applied to the development of a tailored synthetic strategy that cannot be approached by general methods.

Conclusions

The 3,3′-Py_2S ligand is a fascinating tectonic unit without any particular strain in the formation of a helical structure. The ligating nature of the (counter)anion may be a crucial obstacle in the formation of helical molecules. Our results clearly demonstrate that the construction of helical arrays can be induced by anion exchange. The construction and induction of molecular helices are intended to contribute to the development of useful molecular-based materials such as sensors, molecular switches,[15,30] ion exchangers, chemical delivery, and intercalators.

Acknowledgment. This work was supported in part by the Ministry of Science and Technology in Korea.

Supporting Information Available: Crystallographic data for [Ag(3,3′-Py_2S)NO_3], [Ag(3,3′-Py_2S)]BF_4, [Ag(3,3′-Py_2S)]ClO_4, and [Ag(3,3′-Py_2S)]PF_6 and X-ray powder diffraction patterns of [Ag(3,3′-Py_2S)]PF_6 (by the reaction of $AgPF_6$ with 3,3′-Py_2S, by the anion exchange of [Ag(3,3′-Py_2S)]BF_4 with $NaPF_6$, and by the anion exchange of [Ag(3,3′-Py_2S)NO_3] with $NaPF_6$. This material is available free of charge via the Internet at http://pubs.acs.org.

IC001072U